Electron Microscopy of DNA Cross-linked with Trimethylpsoralen: A Probe for Chromatin Structure†

Thomas Cech,‡ David Potter, and Mary Lou Pardue*

ABSTRACT: Me_3psoralen (4,5′,8-trimethylpsoralen) undergoes a photochemical reaction with DNA, resulting in the formation of covalent monoadducts and interstrand cross-links. DNA was photoreacted with [^{3}H]Me_3psoralen inside mouse liver nuclei to the extent of one covalently bound Me_3psoralen molecule per 114 or per 246 base pairs on the average. DNA purified from these nuclei was prepared for electron microscopy under totally denaturing conditions. Adjacent cross-links in the DNA were found to be separated by intervals of 190 base pairs, or by integral multiples of that length. Deproteinized mouse DNA was also photoreacted with [^{3}H]Me_3psoralen under the same conditions. Electron microscopic measurements of the distances between adjacent cross-links in this DNA did not give the discrete distribution seen in the DNA photoreacted in nuclei. Instead, the pattern of cross-links was consistent with a random distribution of Me_3psoralen reaction sites in the DNA. The Me_3psoralen photoreaction of DNA in intact mouse sperm (where protamines have replaced histones) also resulted in an approximately random distribution of cross-links. The discrete cross-linking pattern generated by the photoreaction of DNA in mouse nuclei therefore seems to reflect the periodicity of proteins in chromatin (the nucleosome subunits), as previously suggested by C. V. Hanson et al. [(1976), *Science 193*, 62–64]. These methods should allow the mapping of the in vivo location of nucleosomes on transcriptionally active and inactive DNA and on newly replicated DNA.

The basic repeating subunit of chromatin, the nucleosome, contains 8 histone proteins and about 200 base pairs of DNA (Kornberg, 1974; Van Holde et al., 1974; Weintraub et al., 1975). Nucleosomes serve the structural role of packing DNA into a chromatin fiber. It is not known whether nucleosomes also have a role in the regulation of transcription. *Tetrahymena* and *Xenopus* ribosomal RNA genes (Mathis and Gorovsky, 1976; Reeder, 1975; Reeves, 1976), duck reticulocyte hemoglobin genes (Axel et al., 1975; Weintraub and Groudine, 1976), and hen oviduct ovalbumin genes (Garel and Axel, 1976), all presumably in a state of transcriptional activity, are protected from micrococcal nuclease digestion to the extent expected for a nucleosome structure (Axel et al., 1974). Foe et al. (1976) have observed nucleosomes on active nonribosomal transcription units by electron microscopy. None of these experiments has been detailed enough to determine whether nucleosomes occupy specific positions on or near a transcribed gene, or are randomly distributed.

One useful method for mapping the positions of nucleosomes on DNA may be provided by the psoralen cross-linking reaction. Psoralen and its derivatives are small, heterocyclic molecules that intercalate in DNA. Long wavelength ultraviolet light (360 nm) produces photochemical reactions between psoralens and pyrimidine bases in the DNA. When one psoralen molecule reacts with two pyrimidines on opposite strands of the double helix, a stable, covalent cross-link is formed between the two polynucleotide strands (Musajo and Rodighiero, 1970; Cole, 1971). The photochemical cross-linking of DNA with psoralen compounds can be done in vivo in intact organisms, in tissue culture cells, or in isolated nuclei (Pathak and Kramer, 1969; Cole, 1970; Musajo and Rodighiero, 1970).

Hanson et al. (1976) first investigated the sites in chromatin that are available for photochemical cross-linking with Me_3psoralen. They treated *Drosophila* embryo nuclei with Me_3psoralen plus light, isolated the DNA, and located the Me_3psoralen cross-links by electron microscopy of the DNA under totally denaturing conditions. Hanson et al. concluded that 60% of the DNA was protected from cross-linking except at intervals of 160–200 base pairs and intervals of twice that length. The periodicity of the cross-links suggested that Me_3psoralen reacts mainly with the DNA between nucleosomes. This interpretation was recently substantiated when it was shown that the regions of DNA in nuclei that react most with Me_3psoralen are the same internucleosome segments of DNA preferentially degraded by micrococcal nuclease (Wiesehahn et al., 1977; Cech and Pardue, 1977). Therefore, to a first approximation, the Me_3psoralen cross-links in the purified DNA show the previous locations of nucleosomes in the chromatin.

In the present study we further investigate the electron microscopic mapping of Me_3psoralen cross-links in DNA. The distribution of cross-links in DNA photoreacted in mouse nuclei is compared with the distribution of cross-links in DNA photoreacted after deproteinization or photoreacted in mouse sperm. We also reexamine the conclusion of Hanson et al. (1976) that 40% of the DNA in nuclei (DNA which appears double-stranded even under totally denaturing conditions) is not protected from Me_3psoralen cross-linking. The results presented here will hopefully form the basis for further studies in which Me_3psoralen cross-linking and electron microscopy will be used to map the in vivo positions of nucleosomes on specific DNA sequences, such as ribosomal RNA genes.

Materials and Methods

Isolation of Nuclei. Balb/c and 129/S_v mice were provided by M. Kamarck and S. Epstein. Their livers were dissected and weighed, 1 g of wet liver yielded about 1.2 mg of purified DNA. All subsequent steps were done in an ice bath or a 4 °C cold room. The livers were minced in buffer A containing 1.3 mM

† From the Department of Biology, Massachusetts Institute of Technology, Cambridge, Massachusetts 02139. *Received July 13, 1977.* The investigation was supported by Grant No. CA05178, awarded by the National Cancer Institute, Department of Health, Education and Welfare, and by a grant from the National Science Foundation to M.L.P.

‡ Present address: Department of Chemistry, University of Colorado, Boulder, Colorado 80309.

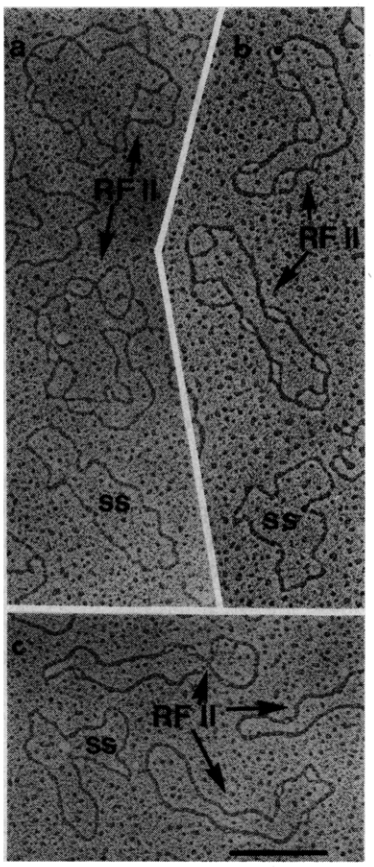

FIGURE 1: ϕX174 RFII DNA photoreacted with Me$_3$psoralen and spread for electron microscopy under totally denaturing conditions. The double-stranded ϕX174 RFII DNA was irradiated in the presence of 3 μg/mL Me$_3$psoralen for (a) 8 min, (b) 20 min, (c) 100 min. The single-stranded (ss) ϕX174 DNA was not present during the photoreaction, but was added before glyoxal denaturation. The length of the bar corresponds to 1000 bases, calculated from the length of the single-stranded ϕX174 DNA.

EDTA and 0.3 mM EGTA.[1] Our buffer A was similar to that of Hewish and Burgoyne (1973), but was made two-thirds as concentrated to avoid the extremely shrunken nuclei we observed with full-strength buffer. The buffer A used here contained 0.22 M sucrose, 10 mM Tris buffer, 10 mM NaCl, 0.67 mM dithiothreitol, 0.33 mM spermidine, 0.10 mM spermine and was adjusted to pH 7.4 with HCl. The minced livers were gently homogenized (Dounce homogenizer, loose "A" pestle), filtered through four layers of cheesecloth, and centrifuged in siliconized tubes for 10 min at 4000 rpm in a Sorvall HB-4 rotor, 0 °C. Gentle homogenization followed by centrifugation was repeated twice in buffer A containing 0.1 mM EDTA, 0.1 mM EGTA, and 0.17% Triton X-100, then once in buffer A. After the last centrifugation, the nuclei were resuspended in buffer A for irradiation.

Isolation of DNA. DNA was isolated from mouse liver nuclei by sodium dodecyl sulfate lysis, proteinase K digestion, and phenol-chloroform extraction as described by Cech and Pardue (1977). The growth of SVT2 mouse tissue culture cells and the isolation of their DNA by a pH 10.5 procedure was described by Cech et al. (1973).

DNA was isolated from mouse sperm by the following method. Sperm were pelleted in a clinical centrifuge and resuspended in 0.01 × SSC–1 mM EDTA. Five volumes of 6 M urea–0.4 M guanidinium hydrochloride–1% β-mercaptoethanol–0.01 M NaH_2PO_4, pH 7, was added to release the DNA from the sperm nuclei, but instead resulted in the precipitation of the DNA. The precipitate was washed in phosphate-buffered saline, dissolved at 65 °C by the addition of 1% sarkosyl, and digested for 4 h at 50 °C with 100 μg/mL Pronase. The DNA was further purified by chloroform extractions and ethanol precipitation.

Photoreaction of DNA with Me$_3$psoralen. [^{3}H]Me$_3$psoralen (72 000 cpm/μg) was a gift of S. T. Isaacs and J. E. Hearst. After addition of Me$_3$psoralen, purified DNA was irradiated in plastic tissue culture flasks (Falcon) and mouse nuclei were irradiated in siliconized glass Petri dishes, using a 0.72 mW/cm^2 long wavelength ultraviolet fluorescent lamp (Cech and Pardue, 1976). The amount of [^{3}H]Me$_3$psoralen covalently bonded with DNA was determined from the specific activity of the DNA after unbound Me$_3$psoralen and its photolysis products had been removed (Cech and Pardue, 1977). Removal of Me$_3$psoralen that has not reacted with the DNA requires several chloroform–isoamyl alcohol extractions with the aqueous phase ionic strength $\geq$0.15 M NaCl (Isaacs et al., 1977).

Electron Microscopy. DNA was denatured in the presence of glyoxal and spread for electron microscopy exactly as described by Cech and Pardue (1976). Single-stranded ϕX174 DNA, added to the samples before glyoxal denaturation, served as a molecular weight standard. It was taken to have a molecular weight of 5250 bases, although 5375 bases is now known to be a more accurate value (Sanger et al., 1977). Grids were scanned and photographed on glass plates with a JEM 100B electron microscope. Photographs were printed at a final magnification of 80 000×. Molecules were measured with the aid of a Numonics electronic graphics calculator interfaced to a PDP 9 computer. The size of denatured bubbles was calculated from the average of the lengths of the two halves of the bubble. (A bubble with two halves each 200 bases in length is said to have a size of 200 bp.) The lengths of bubble regions were taken to be directly proportional to the length of the ϕX standard, while the lengths of apparent double-stranded regions were taken to have a length per bp 1.07 times that of the ϕX standard (see first section of Results).

Results

Calibration of the Length per Base Pair for Me$_3$psoralen Cross-linked DNA. Electron microscopy of DNA under totally denaturing conditions can be used to determine the distance between interstrand Me$_3$psoralen cross-links in the DNA (Hanson et al., 1976; Cech and Pardue, 1976). Earlier studies have assumed that the Me$_3$psoralen photoreaction has a negligible effect on the contour length of DNA under denaturing conditions. To investigate this point, double stranded ϕX174 RFII DNA was cross-linked to different extents. The cross-linked DNA was then mixed with single-stranded ϕX174 DNA as an internal length standard, and the DNAs were totally denatured in the presence of glyoxal and spread for electron microscopy.

Figure 1 shows examples of electron micrographs of the totally denatured ϕX174 molecules. After 8 min of irradiation, the photoreacted DNA appears as a series of single-stranded bubbles (Figure 1a). The bubbles are interpreted to be uncross-linked stretches of DNA bounded by covalent cross-links. Although some bubbles may be formed by the random overlapping of denatured strands, we have previously shown that there is a good correlation between the number of covalent cross-links in DNA, determined by renaturation experiments,

[1] Abbreviations used: EDTA, (ethylenedinitrilo)tetraacetic acid; EGTA, [ethylenebis(oxyethylenenitrilo)]tetraacetic acid; SSC, 0.15 M NaCl–0.015 M sodium citrate; bp, base pair; ds, double-stranded; ϕX174 RFII, nicked double-stranded replicative form of bacteriophage ϕX174 DNA.

TABLE I: Contour Length of Circular ϕX174 DNA Cross-linked with Me_3psoralen[a] and Spread for Electron Microscopy under Totally Denaturing Conditions.

Irrad t (min)	Wt fraction of ϕX RFII DNA in app ds regions[b]	$\bar{L}$ (μm)[c] ϕX RFII[d]	$\bar{L}$ (μm)[c] ss ϕX[e]	Ratio $\bar{L}$(RFII)/$\bar{L}$(ss)
8	0.10 ± 0.08[f]	1.57 ± 0.07[f]	1.46 ± 0.07[f]	1.07
20	0.46 ± 0.13	1.62 ± 0.08	1.48 ± 0.08	1.09
100	0.80 ± 0.07	1.79 ± 0.09	1.60 ± 0.09	1.12

[a] ϕX174 RFII DNA in 0.10 M NaCl–0.05 M sodium phosphate buffer–0.002 M EDTA, pH 6.9, was irradiated for the indicated time in the presence of 3 μg/mL Me_3psoralen. [b] The remainder of the DNA occurred as bubble regions; app, apparent. [c] An average of 56 molecules was measured in each category. [d] Contour length is the average of two measurements: one in which the inner half of each denatured bubble was traced, and one in which the outer half was traced. [e] ss (single-stranded) ϕX174 DNA was not present during the cross-linking reaction, but was added before glyoxal denaturation as an internal length standard. [f] (±) standard deviation.

and the number of regions of intersection of denatured DNA strands in such electron micrographs (Cech and Pardue, 1976). In the more heavily cross-linked DNA shown in Figures 1b and 1c, an increasing fraction of the DNA occurs as apparently double-stranded (ds) regions. These are more heavily stained than the denatured bubbles, and they resemble double-stranded DNA spread under nondenaturing conditions. The apparent ds regions are interpreted to contain bubbles of a size below the limit of resolution of this electron microscopy method (see Discussion).

Table I summarizes the measurements of several hundred molecules like those shown in Figure 1. Because the measured length of identical DNA samples often varies from one electron microscopic preparation to another, we calculate the ratio of the length of the cross-linked molecules to the length of the single-stranded molecules present on the same grid. Over a wide range in the extent of cross-linking of the DNA, the contour length per DNA base pair is the same within 12% for glyoxal-denatured, cross-linked ϕX174 RFII DNA as for glyoxal-denatured single-stranded ϕX174 DNA. The length ratio increases by 0.05 (from 1.07 to 1.12) when the cross-linked DNA increases from 10 to 80% apparent double strandedness. Apparent ds regions are therefore taken to have a length per base pair 7% (1.12–1.07/0.80–0.10) longer than that of the single-stranded ϕX standard.[2]

DNA Photoreacted with Me_3psoralen in Mouse Nuclei. Mouse liver nuclei were isolated by a modification of the procedure of Hewish and Burgoyne (1973) and were photoreacted with [^{3}H]Me_3psoralen to different extents, as described in Materials and Methods section. The irradiation treatment was carried out at 4 °C. DNA isolated from the nuclei was spread for electron microscopy under totally denaturing conditions, as shown in Figure 2. As with the ϕX174 DNA, the more extensively photoreacted mouse DNA contains smaller bubbles (a smaller average distance between cross-links), and a larger fraction of apparently double-stranded regions (Table II). Table II also gives the average amount of photoreaction in each DNA sample, calculated from the specific activity of the DNA after unbound [^{3}H]Me_3psoralen and its photolysis products had been removed. The total amount of ^{3}H radioactivity bound to the DNA includes [^{3}H]Me_3psoralen monoadducts as well as covalent cross-links, although only the latter are detected by electron microscopy.

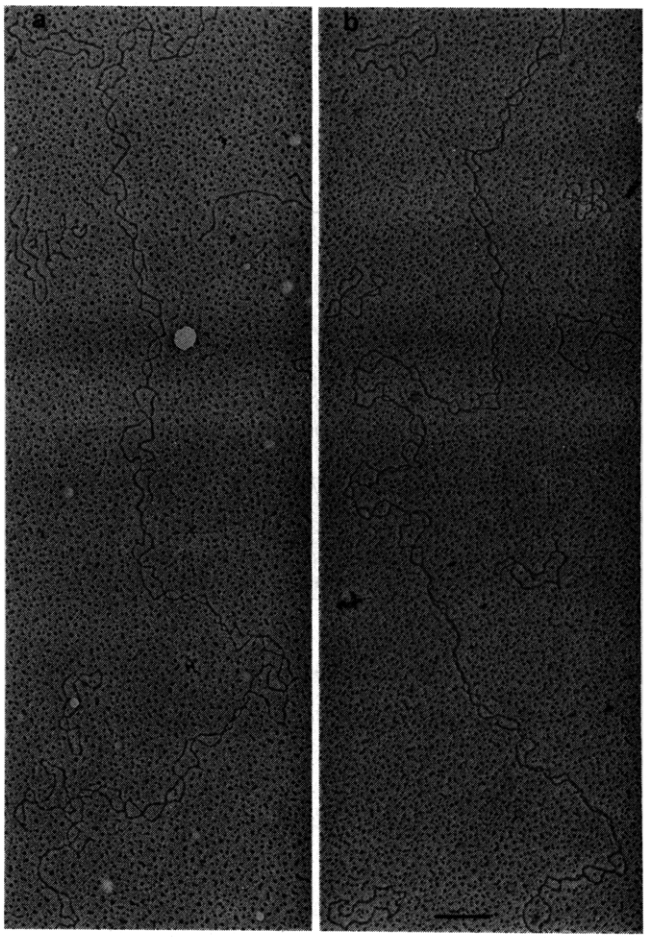

FIGURE 2: Mouse DNA photoreacted with Me_3psoralen in nuclei and spread for electron microscopy after denaturation in the presence of glyoxal. (a) DNA from nuclei irradiated for 38 min in the presence of 6 μg/mL [^{3}H]Me_3psoralen; one Me_3psoralen covalently bound/246 bp. (b) DNA from nuclei irradiated 3 × 15 min with [^{3}H]Me_3psoralen (4 μg/mL) added before each irradiation; one [^{3}H]Me_3psoralen molecule covalently bound/114 bp. Single-stranded circles are ϕX174 DNA. The length of the bar corresponds to 1000 bases.

The solid-line histograms of Figure 3a show the distances between Me_3psoralen-accessible sites in DNA in nuclei. The lengths of the un-cross-linked bubbles occur in discrete size classes. In the less highly cross-linked DNA of Figure 3a, the predominant size classes are centered at 210 and 420 bp (base pairs), with minor classes at higher numbers of base pairs. The predominant size classes in the more extensively cross-linked DNA in Figure 3b are slightly smaller, with peaks at 190 and 390 bp. A higher fraction of the bubbles is in the small size class in Figure 3b.

From the graph of bubble size as a function of peak number in Figure 3c, the bubble sizes are seen to form an arithmetic series based on a "monomer" molecular weight of about 190

[2] The increase in contour length as a function of cross-link density cannot be attributed to "unwinding" of the DNA caused by Me_3psoralen molecules between the bases, because (1) measurements of these same cross-linked ϕX174 RFII DNAs under nondenaturing conditions showed no detectable lengthening compared with un-cross-linked ϕX174 DNA; and (2) the estimated extent of photoreaction for these samples is in the range of 1 Me_3psoralen/250 bp after 8 min of irradiation to 1/75 bp after 100 min, too low to expect detectable lengthening. We believe that the increased length of cross-linked DNA in the glyoxal spreading method can be attributed to the special type of cytochrome *c*–denatured DNA complex that is visualized as an apparent ds region. The apparent ds regions often occur as stiff, rod-like segments, and the DNA in these regions is probably slightly more stretched than that in the bubble regions.

TABLE II: The Extent of Photoreaction of Mouse DNA Treated with [^{3}H]Me$_3$psoralen plus Light.

State of DNA during reaction	Av. no. of bp between Me$_3$-psoralen adducts[a]	Electron microscopy[b] Type of region	Wt fraction of the DNA in each type of region	Av. distance between cross-links (bp)	Ratio of cross-links to covalently bound Me$_3$-psoralen[d]
Nuclei (Figure 2a)	246	Bubble	0.83	528	0.67
		App ds	0.17	~150[c]	
Nuclei (Figure 2b)	114	Bubble	0.72	374	0.43
		App ds	0.28	~150[c]	
Protein free (Figure 4b)	109	Bubble	0.56	376	0.48
		App ds	0.44	~150[c]	

[a] Calculated from the ^{3}H specific activity, and therefore includes monoadducts plus cross-links. [b] DNA was mounted for electron microscopy under totally denaturing conditions, and the lengths of single-stranded regions (bubbles) and of apparently double-stranded (app ds) regions were measured. A total of 2.97×10^5 bp of DNA was measured in sample 2a, 6.87×10^5 bp in 2b, 6.71×10^5 bp in 4b. [c] We estimate a probability of <0.5 for observing a bubble composed of <150 bp (see Figure 5c and text). Bubbles smaller than this limit of resolution would usually appear as ds regions even though the DNA were totally denatured. [d] Calculated as (0.83/528 + 0.17/150)/(1/246) for 2a, (0.72/374 + 0.28/150)/(1/114) for 2b, (0.56/376 + 0.44/150)/(1/109) for 4b. The calculation assumes that each crossover of two DNA strands contains exactly one cross-link, and that ds regions contain one cross-link/150 bp. If the average distance between cross-links in ds regions were much less than 150 bp, then this ratio would exceed 1.0 (which is impossible).

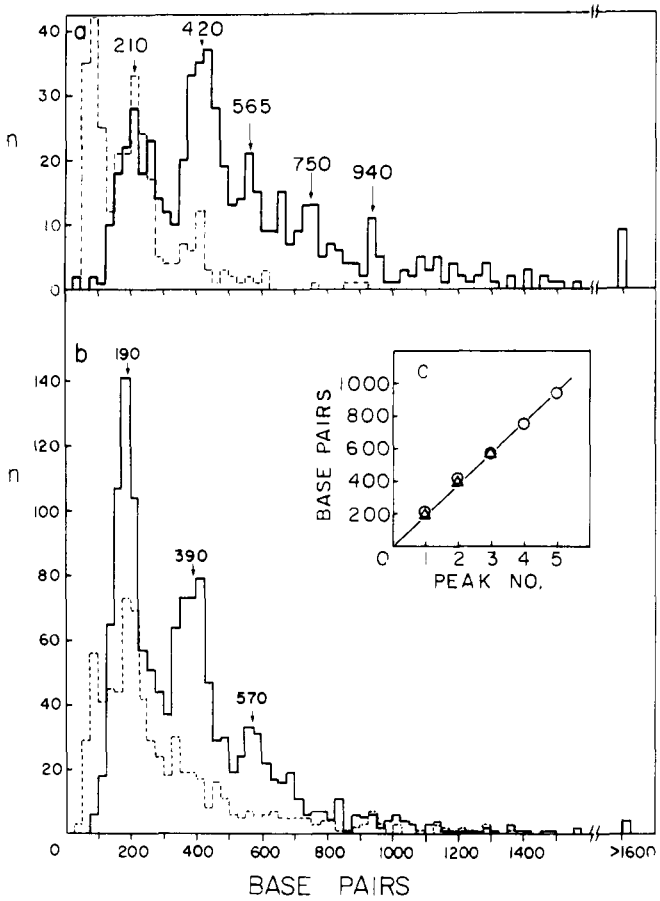

FIGURE 3: Size distributions of un-cross-linked regions and apparently double-stranded regions in DNA photoreacted in intact nuclei. (a) DNA shown in Figure 2a, 1 Me$_3$psoralen/246 bp. (—) Histogram of 563 denatured bubbles. Numbers indicate peaks (mean position ± half-width): 210 ± 60, 420 ± 60, 565, 750, 940 bp. (Insufficient data for determination of half-widths for peaks > dimer.) ϕX174 single-stranded circles, 48, were measured as an internal standard (7.9% relative standard deviation). (- - -) Histogram of 288 apparently ds regions on the same molecules as the above. (b) DNA shown in Figure 2b, 1 Me$_3$psoralen/114 bp. (—) Histogram of 1317 denatured bubbles. Peaks = 190 ± 35, 390 ± 52, 570 bp. ϕX174 circles, 77, were measured as an internal standard (5.9% rel standard deviation). (- - -) Histogram of 692 apparently ds regions on the same molecules. (c) The positions of the peaks of bubble sizes are plotted vs. the peak number. (○) a; (△) b. The line has a slope of 190 bp.

bp. This is the expected periodicity if Me$_3$psoralen reacted mainly with the DNA between nucleosomes, or if it reacted at a constant point within each nucleosome. The average spacing of nucleosomes in rodent liver nuclei has been estimated from micrococcal nuclease digestion experiments as 196 bp (Compton et al., 1976), 198 bp (Noll, 1976), and 196 bp (Cech and Pardue, 1977).

The histograms of Figure 3 resemble in several other ways the distribution of fragment sizes produced by limited nuclease digestion of nuclei. If the histogram of apparently double-stranded regions and the histogram of denatured regions are added, then the number of DNA segments in each peak decreases in the order monomer > dimer > trimer, for the distributions in both Figures 3a and 3b. At the higher amount of photoreaction, there is an increased ratio of the number of DNA segments in the monomer peak relative to the number in the dimer and higher multimer peaks. The positions of the monomer and dimer peaks shift by 20–30 bp at the higher amount of photoreaction, giving an indication of the size of the region that is accessible to Me$_3$psoralen.

An additional similarity—the breadth of the peaks—is fortuitous. The broad peaks observed in the gel electrophoresis of micrococcal nuclease digestion products are due to heterogeneity in DNA fragment size (Noll, 1974). The breadth of the histogram peaks, on the other hand, is dominated by the random variability of DNA lengths that is intrinsic to the basic protein film method of electron microscopy. Based on the standard deviation of 5.9% measured for denatured ϕX174 DNA, the equation of Davis et al. (1971) predicts a standard deviation of 41 bp for a 190-bp bubble and 59 bp for a 390-bp bubble. (For the purpose of the calculation, a 190-bp bubble is considered to be a 380-base single-stranded DNA circle.) The observed half-widths of the histogram peaks, given in the legend to Figure 3, are equal to those predicted. This intrinsic length variability is large enough to obscure a considerable amount of variation in the sizes of the bubbles. For example, if measurements of a homogeneous population of denatured bubbles of size L give a standard deviation σ_s = 40 bp, then by allowing the size of the bubbles to vary continuously in the range $L \pm 40$ bp the half-width of the distribution would only increase to 49 bp. The electron microscopy is therefore not very sensitive to heterogeneity in the size of the chromatin subunits.

Adjacent denatured bubbles most frequently intersected at a single point, with no visible ds (double-stranded) region between them. In other instances, denatured bubbles were separated by what appeared to be double-stranded regions. The lengths of these ds regions are shown in the dashed histograms of Figure 3a,b. Because apparent ds regions of short length occurred even in overlapping sections of the single-stranded ϕX174 marker DNA, the ds regions of length of ~100 bp cannot be considered significantly different from ds regions of zero length. Apparent double-stranded regions longer than 100 bp are less likely to arise by chance; they fall mainly into the same 200 and 400 bp size classes as the single-stranded bubbles. Therefore, the ds regions as well as the bubble regions have a length distribution that suggests a relationship to chromatin structure. (See Discussion.)

Purified Mouse DNA Photoreacted with Me$_3$psoralen. The Me$_3$psoralen cross-linking of protein-free mouse DNA was studied to determine if the 200 base pair periodicity of cross-links might possible be a property of the mouse DNA base sequence or the binding of the spermine and spermidine in the buffer, rather than a result of nucleosome structure. Deproteinized SVT2 mouse tissue culture cell DNA was photoreacted with [^{3}H]Me$_3$psoralen using different times of irradiation to control the extent of reaction. The buffer conditions, temperature, and DNA concentration were identical with those used in the photoreaction of the mouse nuclei. The use of mouse tissue culture cell DNA rather than mouse liver DNA is not a significant difference: the SVT2 cells have a normal mouse karyotype and their DNA cross-hybridizes with mouse liver DNA (Cech and Hearst, 1976).

The extent of Me$_3$psoralen cross-linking was determined by mounting the DNA for electron microscopy under totally denaturing conditions, as shown in Figure 4. The relatively low extent of cross-linking compared with the ϕX174 RFII DNA (Figure 1) can be attributed to the presence of spermine and spermidine in the solution during the photoreaction. These polyamines bind tightly to DNA at low ionic strengths (Tsuboi, 1964; Liquori et al., 1967; Hirschman et al., 1967). Measurements of the distance between points of intersection of DNA strands showed that an average of 2000 bp separated adjacent cross-links in the DNA sample that had been irradiated for 10 min (Figure 4a). The DNA samples irradiated for 60 min (Figure 4b) and 120 min (Figure 4c) showed progressively smaller denatured bubbles, with a corresponding increase in the fraction of the DNA that contained bubbles too small to be resolved (apparent ds regions).

The DNA sample that was given the intermediate amount of photoreaction (Figure 4b) had a cross-linking pattern that appeared very similar to that of one of the samples cross-linked in mouse nuclei (Figure 2b). Table II shows that these two DNA samples have an almost identical extent of photoreaction, determined from tritium radioactivity, and an almost identical average bubble size when denatured and spread for electron microscopy. The distribution of bubble sizes in the cross-linked purified DNA, however, does not show the 200-bp periodically seen when DNA is cross-linked in nuclei. Instead, as shown in Figure 5a, the bubbles have a fairly continuous size distribution with a peak at 250–300 bp. This distribution is that expected for random cross-linking of the DNA (see below).

The size distribution for the apparent ds regions in this DNA is also given in Figure 5a. It shows the same peak at ~100 bp that was seen with the DNA cross-linked in nuclei (Figure 3a,b). As mentioned in the previous section, apparent ds regions of such short length cannot be considered significant. The larger apparent ds regions decrease in number with increased size in a fairly continuous manner, with no evidence of the peaks at 200 and 400 bp that were seen with the DNA photoreacted in nuclei.

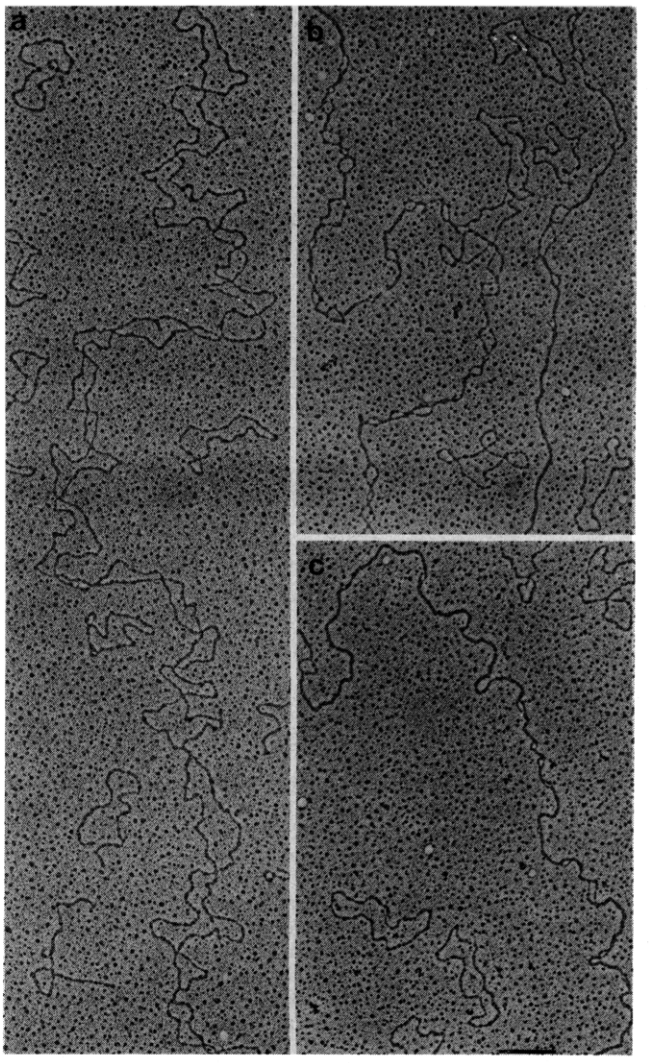

FIGURE 4: Purified mouse DNA photoreacted with Me$_3$psoralen and analyzed by electron microscopy under totally denaturing conditions. Purified DNA was irradiated for (a) 10 min, (b) 60 min, and (c) 120 min in the presence of 6 μg/mL [^{3}H]Me$_3$psoralen. A second 6 μg/mL [^{3}H]-Me$_3$psoralen was added to sample c at 60 min of irradiation. The single-stranded circles are ϕX174 DNA; the length of the bar corresponds to 1000 bases.

A Simple Theory for Random Cross-linking of DNA. We assume that the formation of one covalent cross-link in the DNA does not affect the formation of subsequent cross-links: that is, that cross-links are independent events. Electron micrographs of DNA with a low extent of cross-linking, such as that shown in Figure 4a, show the cross-links to be widely scattered rather than clustered. This provides good evidence against a high degree of cooperativity for Me$_3$psoralen cross-linking. The assumption of independent events must fail at very high degrees of cross-linking, because if the nth nucleotide is cross-linked to the $n + 1$ nucleotide of the opposite strand, it cannot form a cross-link with the $n - 1$ nucleotide.

Let p be the average probability that the nth nucleotide is cross-linked to the $n + 1$ nucleotide of the opposite strand. (The average distance between cross-links is then $1/p$.) We restrict our discussion to low extents of reaction, where $p < 0.02$. The probability of finding x cross-links in a sample of b nucleotides is given by the Poisson distribution as

$$X(x) = (bp)^x e^{-bp}/x! \ (b \text{ an integer} \gg 1, p \ll 1) \quad (1)$$

In the denatured DNA electron micrographs, a bubble of size

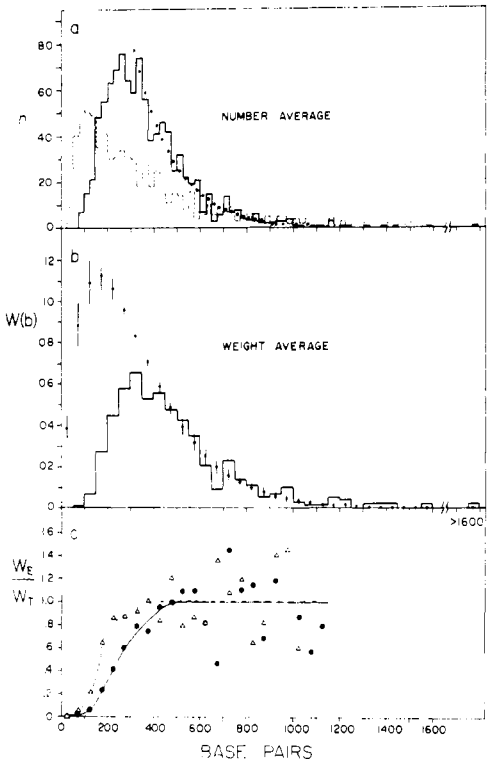

FIGURE 5: Size distributions of un-cross-linked regions and apparently double-stranded regions in mouse DNA that had been deproteinized before photoreaction. An electron micrograph of this DNA is shown in Figure 4b, and it is further characterized in Table II. (a) (—) Histogram of 996 denatured bubbles on 22 randomly chosen molecules. ϕX174 single-stranded circles, 128, were measured as an internal standard (5.4% rel standard deviation). (- - -) Histogram of 748 apparent ds regions on the same molecules. (●) Theoretical distribution from eq 2, $1/p$ = 163 bp. The theory assumes that even the smallest distances between cross-links are detected as bubbles. (b) (—) The bubble size histogram in a is transformed into a weight-average histogram. Histogram intervals are 50 bp instead of the 25 bp used in a. (●) Theoretical histogram of the distance between adjacent cross-links from eq 4, with $1/p$ = 163 bp between cross-links. Each point gives the weight fraction of the DNA in that 50-bp interval. The vertical lines show the effect of varying $1/p$ by ±12 bp. The area under the theoretical histogram is 1.00, corresponding to the entire DNA sample. The area under the experimental histogram is 0.56, the fraction of the DNA in bubble regions. The remaining 0.44 of the DNA was contained in apparent ds regions; if the sizes of bubbles in the region could be measured they would presumably fill in the gap between the experimental and theoretical histograms. The standard error of estimate (S_y) was calculated as a measure of the goodness of fit of the theory: $S_y = (\Sigma(W_T - W_E)^2/h)^{1/2}$, where W_T and W_E are the theoretical and experimental values of $W(b)$ and h is the number of histogram intervals. In the region between 400 and 1600 bp, S_y = 0.0073 and the average value of W_E was 0.0228, so the relative standard error of estimate ($S_y/\langle W_E \rangle$) was 32%. The fit between data and theory is not good enough to exclude the possibility that some of the Me$_3$psoralen cross-links are spaced at discrete intervals and some at random intervals. (c) The ratio of the experimentally observed fraction of bubbles of a certain size to the fraction of bubbles of that size theoretically expected for random cross-linking. (●) Ratio calculated from the histogram in b. (△) Ratio calculated from another experiment in which deproteinized DNA was cross-linked to a similar extent as the DNA in b. We interpret the W_E/W_T ratio as the probability of visualizing a denatured DNA bubble of a certain size. Un-cross-linked regions <100 bp are rarely visualized as bubbles. In the range $100 < b < 300$ there is an increasing probability of an un-cross-linked region being visualized as a bubble rather than being hidden in an apparent ds region. Un-cross-linked regions >300 bp are usually visualized as bubbles: the average value of W_E/W_T is 1.0 in this range. The scatter in the points reflects the limited goodness of fit of the random distribution to the data.

b occurs if $b - 1$ consecutive un-cross-linked nucleotides are followed by a cross-linked nucleotide. The probability of a bubble of size b is therefore

$$P(b) = X(0)p = e^{-(b-1)p}p \approx pe^{-bp} \quad (b \gg 1) \qquad (2)$$

This is the number-average form of the random cross-linking expression. It is converted to the weight-average form $W(b)$ by weighting each bubble by its size b and dividing by the average bubble size ($1/p$):

$$W(b) = bP(b)/(1/p) = bp^2e^{-bp} \qquad (3)$$

For the purpose of calculating the weight fraction of the distribution in a certain histogram interval, the summated form of 3 is useful:

$$\sum_{b=i}^{j} W(b) = -(1 + jp)e^{-jp} + (1 + ip)e^{-ip} \qquad (4)$$

Equation 3 satisfies the normalization condition

$$\sum_{b=0}^{\infty} W(b) = 1 \qquad (5)$$

The electron micrographs allow measurement of the distance between cross-links only in the bubble regions of the denatured molecules; in the apparent ds regions the individual cross-links cannot be visualized. Measurement of the micrographs does, however, give the fraction *by weight* of un-cross-linked stretches of DNA that are hidden in apparent ds regions. This is simply the total number of base pairs in apparent ds regions divided by the total number of base pairs in the sample, determined by contour length measurements. If a bubble size histogram from a randomly cross-linked DNA sample is converted to its weight-average form and then compared with the weight-average form of the random cross-linking expression (eq 4), the two histograms are expected to coincide at high values of b, where un-cross-linked stretches of DNA should be easily visible as denatured bubbles. At lower values of b, when denatured stretches become hidden in apparent ds regions, the theoretical curve will exceed the experimental data. (See Figure 6.)

Figure 5b gives the weight-average bubble-size histogram for the deproteinized mouse DNA that was photoreacted under the same conditions used for nuclei. The best fit of the random cross-linking theory (eq 4) to the histogram occurred with p = 0.0061, which corresponds to 1 cross-link per 163 bp. (From the amount of [^{3}H]Me$_3$psoralen covalently bound to this DNA—one molecule per 109 bp (Table II)—we would predict approximately one cross-link per 220 bp.) The theoretical histogram gives an adequate fit to the data for $b > 300$ bp (see legend to Figure 5), but deviates substantially from the data in the region $b < 300$ bp. The simplest interpretation is that the ratio of the experimental to the theoretical value reflects the probability of visualizing a denatured bubble of that size (Figure 5c). Thus, an un-cross-linked DNA stretch of ~300 bp is visualized as a denatured bubble with a 70% frequency and is hidden in an apparent ds region with a 30% frequency; un-cross-linked stretches of 200 and 100 bp are visualized as bubbles with approximately 35% and 5% efficiencies, respectively. The mean size of an un-cross-linked region in an apparent ds region is calculated to be 150 bp for this sample.

Two other samples of deproteinized mouse DNA were photoreacted for 10 min and 64 min in NaCl–EDTA–sodium phosphate buffer (0.19 M Na^+, pH 6.9) and spread for electron microscopy under denaturing conditions. The weight-average bubble size distributions were again well fit with the random distribution of eq 4 at high values of b, but deviated at values of $b < 250$ bp. (The experimental and theoretical bubble size distributions for the DNA irradiated for 10 min are compared in Figure 5c, triangle symbols.) The correspondence between the experimental bubble size distribution and the expected random distribution is therefore not restricted to the sample analyzed in Figure 5a; nor is it dependent on the

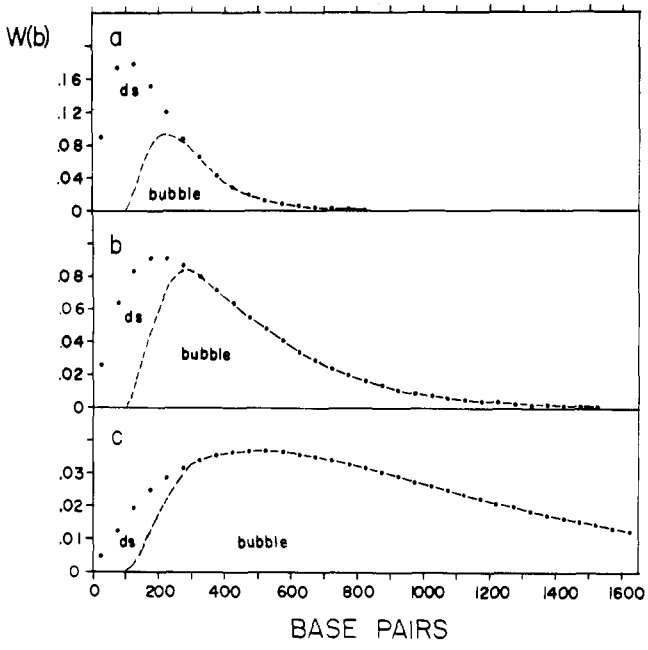

FIGURE 6: Bubble size histograms expected for random cross-linking of DNA. The three curves represent three different extents of random cross-linking of the DNA. (a) An average of one cross-link per 100 bp, $1/p = 100$, $p = 0.010$. (b) One cross-link per 200 bp, $1/p = 200$, $p = 0.005$. (c) One cross-link per 500 bp, $1/p = 500$, $p = 0.002$. (●) The weight fraction of the bubbles in each 50-bp interval, calculated from eq 4. The area under each set of circles is equal to 1.0. (Note the different ordinate scales; also, in curve c 0.17 of the area is off the graph in the region > 1600 bp.) (- - -) The expected shape of the experimental bubble histogram, using Figure 5c to give the probability of visualizing a bubble of each size. As the average frequency of cross-links decreases, a higher fraction of the DNA appears in bubble regions: 0.48 in a, 0.77 in b, and 0.94 in c. The "ds" notation refers to the region of the theoretical cross-linking distribution where the DNA between cross-links is visualized as apparent double-stranded regions rather than as bubbles. The sum of the "ds" and "bubble" areas equals the theoretical cross-linking distribution, designated by the filled circles.

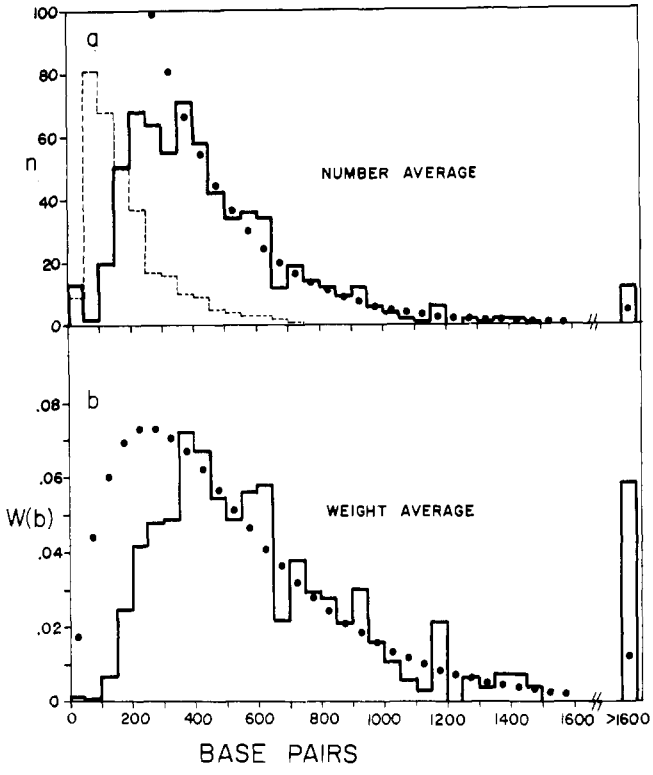

FIGURE 7: Size distributions of un-cross-linked regions and apparent ds regions in DNA photoreacted with Me_3psoralen in mouse sperm. Epididymus tissue was dissected from an 11 week old Balb/c male mouse. To release sperm, the epididymus was minced in Dulbecco's modified Eagle's medium (containing 2% calf serum). Nonradioactive Me_3psoralen was added to a final concentration of 3 μg/mL, and the mixture was irradiated for 120 min at 28 °C in a plastic Petri dish. The sperm were then drawn off with a Pasteur pipet. DNA was isolated and prepared for electron microscopy as described in Materials and Methods. (a) (—) Number-average histogram of 666 denatured bubbles. (- - -) Histogram of 315 apparent ds regions on the same molecules. Total amount of DNA measured was 3.67×10^5 bp. (●) Number average bubble size histogram expected for $1/p = 250$ bp, from eq 2. (b) (—) The bubble size histogram in a is transformed into a weight-average histogram. (●) Theoretical histogram of the distance between adjacent cross-links from eq 4, with $1/p = 250$ bp. The measurements showed that 84% by weight of the DNA was contained in bubbles, 16% in apparent ds regions. Therefore 16% of the area under the theoretical curve is not represented in the experimental bubble-size histogram; some of the bubbles in the 200–350-bp range and most of the bubbles < 200 bp seem to be contained in the apparent ds regions. In the region between 350 and 1600 bp, S_y (see Figure 5 legend) = 0.008 and the average value of $W(b) = 0.029$, so the relative standard error of estimate was 28%.

presence of spermine and spermidine during the photoreaction.

DNA Photoreacted with Me_3psoralen in Mouse Sperm. Protamines—small polypeptides rich in arginine—replace histones during spermiogenesis in the mouse (Kierszenbaum and Tres, 1975; Lam and Bruce, 1971). Bellvé et al. (1975) have shown that there are two mouse protamines with similar molecular weights. These two protamines contain 36 and 38 basic amino acids (arginine, histidine, and lysine) of a total of approximately 50 residues (A. R. Bellvé and R. Carraway, personal communication). Because nucleoprotamine complexes are impervious to micrococcal nuclease digestion (Honda et al., 1974), we used Me_3psoralen cross-linking to investigate the arrangement of protamines on DNA in sperm.

Figure 7 shows the distribution of Me_3psoralen cross-links that resulted from the photoreaction of DNA in intact mouse sperm. The low extent of cross-linking could be due to protamines protecting the DNA from Me_3psoralen intercalation, or to some other factor such as reduced penetration of the drug into sperm heads. The weight-average distribution (Figure 7b) was compared with the random cross-linking distribution at molecular weights >350 bp in the same manner described for the deproteinized DNA sample in Figure 5b. Although there appeared to be some preferential quantization of bubbles at 600 bp, the goodness of fit of the random distribution to the sperm DNA data was slightly better than that of the deproteinized DNA data. We conclude that the Me_3psoralen cross-linking of DNA in mouse sperm occurs predominantly at randomly located sites.

Based on its content of basic amino acids, each protamine might protect 18–19 bp of DNA from Me_3psoralen. In that case, our electron microscopy technique would not resolve the individual units of protection, and the cross-linking would appear random. If there were higher order structures such as protamine multimers that protected regions of DNA greater than ~150 bp, they could have been detected.

Discussion

Mouse nuclei and deproteinized mouse DNA were photoreacted with Me_3psoralen under the same conditions, and the distributions of cross-links in the DNAs were compared.

Cross-linking of Deproteinized DNA. In the DNA that was deproteinized before photoreaction, the cross-link distribution was consistent with the random location of Me_3psoralen re-

action sites[3] in the DNA. At the resolution of electron microscopy, the cross-linking would appear random if regions 50 bp in size contained approximately equal numbers of reaction sites. Portions of the mouse genome that contain substantial polypyrimidine stretches are expected to form larger uncross-linked regions than predicted by the random theory. However, long pyrimidine tracts and their complementary purine tracts comprise only 1–1.5% of the mouse genome (Straus and Birnboim, 1974), not enough to noticeably shift the Me_3psoralen cross-linking distributions.

Cross-linking of DNA in Nuclei. When DNA was photoreacted with Me_3psoralen in intact mouse nuclei, adjacent cross-links were not randomly distributed but were separated by integral multiples of a 190-bp unit length (Figure 3). Our results are in basic agreement with those of Hanson et al. (1976), who photoreacted DNA with Me_3psoralen in *Drosophila* embryo nuclei. Like Hanson et al., we suggest that the uniform spacing of the Me_3psoralen cross-links is due to the periodicity of groups of histone proteins in chromatin. Recent nuclease digestion studies (Cech and Pardue, 1977; Wiesehahn et al., 1977) have confirmed that the major site of Me_3psoralen reaction is with the DNA most susceptible to micrococcal nuclease, i.e., the DNA between nucleosomes.

The electron micrographs of DNA cross-linked in mouse nuclei (Figure 2) or *Drosophila* nuclei (Hanson et al., 1976) contain apparent ds regions as well as denatured bubbles. Hanson et al. suggested that apparent ds regions might result from a high frequency of cross-linking in the same portions of the chromatin that are highly accessible to nucleases. Our data do not support this view. The ratio (Table II) of the number of cross-links seen in the electron microscope to the number of Me_3psoralen molecules bound to a DNA sample, determined from tritium radioactivity, is too high to permit a large number of cross-links being hidden in ds regions. The length distributions of the apparent ds regions, given in the dashed-line histograms in Figure 3, have peaks at the same positions as those in the bubble histograms: 200 and 400 bp. This suggests that the apparent ds regions could result from the collapse of some of the denatured bubbles that are approximately 200 bp in size, and the collapse of a smaller fraction of the larger bubbles. Alternatively, there could be a class of nucleosomes in the chromatin that have a site accessible to Me_3psoralen at or near their middle as well as at both ends. If an un-cross-linked region of 200 bp received a single additional cross-link in the middle, electron microscopy of the DNA would resolve the 100-bp bubbles with a low efficiency. In any case, the occurrence of ds regions does not necessarily imply the existence of highly accessible (e.g., protein-free) regions of chromatin.

Because there is a decreased probability of visualizing denatured DNA bubbles smaller than 300 bp, the bubble size histograms of DNA cross-linked in nuclei are expected to be inaccurate in the low molecular weight range. These histograms (Figure 3) can be corrected by using the graphs in Figure 5c to estimate the fraction of the bubbles in each histogram interval that was not detected. The correction has no substantial effect on either the size or the position of the "dimer" peaks, centered at ~400 bp. The number of data points in the 200 bp "monomer" peaks, however, increases by a factor of 2–3, depending on which of the two correction curves in Figure 5c is applied. The center of each monomer peak appears to shift by about 25 bp toward a lower molecular weight. This shift is caused by an increase in the 100–150 bp region of the histogram, where the correction curves are based on very little data and may therefore be inaccurate. Alternatively, we can compensate for the decreased probability of visualizing small denatured bubbles by adding the histogram of apparent ds regions to the histogram of denatured bubbles. This method assumes that the "lost" bubbles have collapsed to form apparent ds regions of the same size, and ignores the possibility that two adjacent bubbles could collapse to form one ds region. When applied to the histograms of Figure 3, this second method of correction again has little effect on the dimer peaks, but approximately doubles the number of data points in the monomer peaks. The positions of the monomer peaks are not detectably changed when this second method of correction is employed. We conclude that the main effect of the decreased probability of visualizing small denatured bubbles on the histograms of Figure 3 is to underestimate the number of monomer-sized bubbles.

Visualizing Small Denatured Regions of DNA in the Electron Microscope. The detection of small single-stranded bubbles in DNA spread for electron microscopy by the protein monolayer technique has been a problem in experiments in addition to those described here. For instance, in their study of T7–T3 heteroduplexes, Davis and Hyman (1971) found that single-stranded loops 100 bp in size were not consistently observed, due to the collapse of a large amount of cytochrome *c* around the DNA. We have compared (Figures 5 and 6) the experimental cross-linking distributions of deproteinized DNA with the distribution expected for random cross-linking. Although denatured regions of size ~100 bp are sometimes seen, the majority of the bubbles of this size appear to be collapsed under our spreading conditions to form apparent ds regions. We find that not even all of the bubbles of size ~200 bp are detectable, and only bubbles >300 bp are visualized with high efficiency. We cannot, however, extend these conclusions beyond the total denaturation method of preparing DNA for electron microscopy. Other variations of the protein monolayer method, particularly those in which less cytochrome *c* is bound to the DNA, may allow the more efficient detection of small denatured regions.

Acknowledgments

We thank S. T. Isaacs and J. E. Hearst for gifts of [^{3}H]-Me_3psoralen, D. Levinstone for patient help in computer programming, and I. T. Young and M. Eden for use of the computer facilities of the MIT Research Laboratory of Electronics.

References

Axel, R., Cedar, H., and Felsenfeld, G. (1975), *Biochemistry 14,* 2489–2495.

Axel, R., Melchior, W., Jr., Sollner-Webb, B., and Felsenfeld, G. (1974), *Proc. Natl. Acad. Sci. U.S.A. 71,* 4101–4105.

Bellvé, A. R., Anderson, E., and Hanley-Bowdoin, L. (1975), *Dev. Biol. 47,* 349–365.

Cech, T. R., and Hearst, J. E. (1976), *J. Mol. Biol. 100,* 227–256.

Cech, T. R., and Pardue, M. L. (1976), *Proc. Natl. Acad. Sci. U.S.A. 73,* 2644–2648.

Cech, T. R., and Pardue, M. L. (1977), *Cell 11,* 631–640.

Cech, T. R., Rosenfeld, A., and Hearst, J. E. (1973), *J. Mol. Biol. 81,* 299–325.

Cole, R. S. (1970), *Biochim. Biophys. Acta 217,* 30–39.

Cole, R. S. (1971), *Biochim. Biophys. Acta 254,* 30–39.

[3] A reaction site for cross-linking is thought to consist of a pyrimidine on one strand of the DNA plus a pyrimidine of an adjacent base pair on the other DNA strand (Cole, 1970; Dall'Acqua et al., 1971). Approximately one-half of all nearest neighbor base pairs in the DNA would then be potential cross-linking sites.

Compton, J. L., Bellard, M., and Chambon, P. (1976), *Proc. Natl. Acad. Sci. U.S.A. 73,* 4382-4386.
Dall'Acqua, F., Marciani, S., Ciavatta, L., and Rodighiero, G. (1971), *Z. Naturforsch. B 26,* 561-569.
Davis, R. W., and Hyman, R. W. (1971), *J. Mol. Biol. 62,* 287-301.
Davis, R. W., Simon, M., and Davidson, N. (1971), *Methods Enzymol. 21,* 413-428.
Foe, V. E., Wilkinson, L. E., and Laird, C. D. (1976), *Cell 9,* 131-146.
Garel, A., and Axel, R. (1976), *Proc. Natl. Acad. Sci. U.S.A. 73,* 3966-3970.
Hanson, C. V., Shen, C.-K. J., and Hearst, J. E. (1976), *Science 193,* 62-64.
Hewish, D. R., and Burgoyne, L. A. (1973), *Biochem. Biophys. Res. Commun. 52,* 504-510.
Hirschman, S. Z., Leng, M., and Felsenfeld, G. (1967), *Biopolymers 5,* 227-233.
Honda, B. M., Baillie, D. L., and Candido, E. P. M. (1974), *FEBS Lett. 48,* 156-159.
Isaacs, S. T., Shen, C.-K. J., Hearst, J. E., and Rapoport, H. (1977), *Biochemistry 16,* 1058-1064.
Kierszenbaum, A. L., and Tres, L. L. (1975), *J. Cell Biol. 65,* 258-270.
Kornberg, R. D. (1974), *Science 184,* 868-871.
Lam, D. M. K., and Bruce, W. R. (1971), *J. Cell. Physiol. 78,* 13-24.
Liquori, A. M., Constantino, L., Crescenzi, V., Elia, V., Giglio, E., Puliti, R., DeSantis Savino, M., and Vitagliano, V. (1967), *J. Mol. Biol. 24,* 113-122.
Mathis, D. J., and Gorovsky, M. A. (1976), *Biochemistry 15,* 750-755.
Musajo, L., and Rodighiero, G. (1970), *Photochem. Photobiol. 11,* 27-35.
Noll, M. (1974), *Nature (London) 251,* 249-251.
Noll, M. (1976), *Cell 8,* 349-355.
Pathak, M. A., and Kramer, D. M. (1969), *Biochim. Biophys. Acta 195,* 197-206.
Reeder, R. H. (1975), *J. Cell Biol. 67,* 357a.
Reeves, R. (1976), *Science 194,* 529-532.
Sanger, F., Air, G. M., Barrell, B. G., Brown, N. L., Coulson, A. R., Fiddes, J. C., Hutchison, C. A., III, Slocombe, P. M., and Smith, M. (1977), *Nature (London) 265,* 687-695.
Straus, N. A., and Birnboim, H. C. (1974), *Proc. Natl. Acad. Sci. U.S.A. 71,* 2992-2995.
Tsuboi, M. (1964), *Bull. Chem. Soc. Jpn. 37,* 1514-1522.
Van Holde, K. E., Sahasrabuddhe, C. G., and Shaw, B. R. (1974), *Nucleic Acids Res. 1,* 1579-1586.
Weintraub, H., and Groudine, M. (1976), *Science 193,* 848-856.
Weintraub, H., Palter, K., and Van Lente, F. (1975), *Cell 6,* 85-110.
Wiesehahn, G. P., Hyde, J. E., and Hearst, J. E. (1977), *Biochemistry 16,* 925-932.

Structure of the 5.8S RNA Component of the 5.8S–28S Ribosomal RNA Junction Complex†

Norman R. Pace,* Thomas A. Walker, and Ellen Schroeder

ABSTRACT: The 5.8S ribosomal RNA of mouse L-cells is dissociable from 28S rRNA by treatment with agents which disrupt hydrogen bonding. The 5.8S-28S rRNA association is restored by appropriate annealing procedures, to yield a complex with thermal denaturation properties identical with those of the native 5.8S-28S rRNA complex. Ribonuclease digestion of the artificial 5.8S-28S rRNA complex, radioactive only in the 5.8S rRNA moiety, yields a fragment not released from uncomplexed 5.8S rRNA. This 5.8S-derived fragment has the properties expected of the 5.8S-28S rRNA junction complex, including ribonuclease resistance, a sharply temperature-dependent reduction in apparent size, and the ability of denatured fragments to reanneal with 28S but not 18S rRNA. The 5.8S-28S rRNA junction complex is shown to include the 3′-terminal 42-43 nucleotides of the 5.8S rRNA molecule; however, it is proposed that only the 3′-terminal 20-21 nucleotides are associated by complementary base interaction with the 28S rRNA. The residuum (21-22 nucleotides) of the 5.8S rRNA component of the junction complex is envisaged to form an intramolecular hairpin which stacks upon and hence stabilizes the RNA double helix formed by the 5.8S-28S association.

It is becoming evident that specific RNA-RNA interactions are of paramount importance to the machinations of the protein-synthesizing apparatus. For example, in prokaryotes 16S ribosomal RNA (rRNA) appears to assist in the binding of mRNA to the ribosome (Shine and Dalgarno, 1971; Steitz and Jakes, 1975); 5S rRNA may be involved in the placement and/or displacement of the tRNA molecules from their sites on the ribosome surface (Erdmann et al., 1973); and structural transitions in the tRNA-mRNA complex have been proposed to provide the essence of the translocation process (Woese, 1970). An example of an RNA-RNA interaction which as yet has no known role is the 5.8S-28S rRNA complex which exists in the ribosomes of eukaryotes (Pene et al., 1968). The 5.8S rRNA, which is about 160 nucleotides in length (Nazar et al., 1975), is rather stably associated along a portion of its length with the 28S rRNA, apparently through hydrogen bonding. The 5.8S-28S rRNA complex is dissociated by heat or urea (Pene et al., 1968), and may be reformed from its constituent

† From the National Jewish Hospital and Research Center, and the Department of Biophysics and Genetics, University of Colorado Medical Center, Denver, Colorado 80206. *Received June 1, 1977.* This work was supported by National Institute of General Medical Sciences Grants GM20147 and GM22367, and Career Development Award No. 1-K04-GM00189 to N.R.P.